

Contents lists available at ScienceDirect

Materials Letters

journal homepage: www.elsevier.com/locate/matlet





The effect of simulated inflammatory conditions on the corrosion of Mg, Fe and CoCrMo

Xiao Liu^a, Wenting Li^b, Yan Cheng^a, Yufeng Zheng^{a,b,*}

- a Academy for Advanced Interdisciplinary Studies, Peking University, Beijing 100871, China
- ^b School of Materials Science and Engineering, Peking University, Beijing 100871, China

ARTICLE INFO

Keywords:
Biodegradable metal
Magnesium
Iron
Simulated inflammatory condition

ABSTRACT

For the first time, the effect of inflammation on the degradation of Mg and Fe was evaluated. The immersion test and electrochemical approaches were carried out under simulated inflammatory condition, with CoCrMo alloy selected as the reference. It turned out that H_2O_2 , the major reactive oxygen species released in the inflammation, changed the surface film behavior of pure Mg and CoCrMo alloy for the initial exposure in PBS, but insignificantly affected their corrosion during the long-term immersion. By contrast, H_2O_2 actively participated in the degradation of pure Fe in a concentration-relevant manner, notably accelerated the Fe corrosion, and inhibited the corrosion product formation during 14-day immersion. It's suggested that inflammation induced corrosion should be taken into consideration in evaluating biodegradable metals.

1. Introduction

Cobalt-based alloys, titanium-based alloys, and stainless steels, with exceptional mechanical properties and corrosion resistance are widely used in cardiovascular and orthopedic devices. However, the usage of inert implants to fulfil the temporary mission might lead to several complications, and a second surgery is required to remove them [1]. Biodegradable metals, expected to gradually corrode in vivo with an appropriate host response, and dissolve completely after healing [2], are thus introduced as promising alternatives in the past decades.

Inflammation is ubiquitous during healing with implant insertion. For inert implants, released debris and ions due to wear or abrasion might invoke adverse inflammatory reactions [3]. The phagocytic cells associated with inflammation could release a variety of reactive oxygen species (ROS) such as hydrogen peroxide (H_2O_2) and superoxide (O_2^-) , creating a locally corrosive environment to attack foreign bodies [4], and possibly affect the metal corrosion. The inflammation-induced corrosion regarding CoCrMo alloy has been studied. Apparent cell-induced corrosion patterns on human-retrieved CoCrMo implant was observed [4], and inflammation-based solution chemistry altered corrosion susceptibility and surface oxide impedance [5]. H_2O_2 , the major ROS released by inflammatory cells, is a strong oxidant [6]. The solution containing H_2O_2 changed the corrosion resistance of metal [7], affected the oxide film behavior on CoCrMo [8], and increased oxide

film instability of pure Ti [9].

Mg and Fe, promising candidates as biodegradable metal, have drawn extensive attention recently. However, inflammation-induce corrosion has never been considered in evaluating their degradation. Besides, Fe ions can engage in Fenton reaction to react with ROS like $\rm H_2O_2$, producing highly oxidative radicals like (OH') to accelerate corrosion, reduce the protection of oxide film and facilitate the corrosion of CoCrMo [5,6]. Biodegradable Fe unceasingly corroded during implantation, possibly contributing to a great amount of hydroxyl radicals [10], which might exert huge impact on its corrosion. Thus, the degradation of Mg and Fe under simulated inflammatory conditions was investigated. Phosphate buffer saline (PBS) with a varying concentration of $\rm H_2O_2$ are prepared for immersion test and electrochemical approaches, and CoCrMo alloy is selected as the counterpart.

2. Experimental

2.1. Sample preparation

Pure magnesium rods (99.98%), pure iron ingots (99.9%) and CoCrMo alloy ingot (ASTM F1537-11) were cut into disks of 10.0 mm in diameter and 1.0 mm in thickness. Specimens were mechanically polished with SiC papers up to 2000 grits, ultrasonically cleaned in acetone and then ethanol, and dried in air.

^{*} Corresponding author at: School of Materials Science and Engineering, Peking University, Beijing 100871, China. E-mail address: yfzheng@pku.edu.cn (Y. Zheng).

2.2. Immersion tests

The simulated inflammatory solutions were prepared by mixing PBS with 0.1 mM, 1.0 mM, or 30.0 mM $\rm H_2O_2$. The initial pH was adjusted to 7.40 with NaOH and HCl. Immersion tests were performed at 37 °C for 1, 3, 7 and 14 days, with a ratio of solution volume to surface area at 20 mL/cm². Solution pH was monitored and recorded.

Samples were taken out after immersion, cleaned with distilled water and dried in air. Surface morphology was characterized by environmental electron microscopy (ESEM, Thermal Fisher Quattro S, USA). The corrosion product was removed by 200 g/L CrO_3 solution. The corrosion rate (mm/yr) can be derived by the following Eq. (1).

Corrosion rate =
$$(K \times W)/(A \times T \times D)$$
 (1)

The coefficient $K=8.76\times 10^4$, W is the weight loss (g), A is the exposed area (cm²), D is the density (g/cm³) and T is immersion time (h).

2.3. Electrochemical experiments

Electrochemical measurements were conducted at 37 $^{\circ}$ C, with an electrochemical workstation (Autolab, Metrohm, Switzerland). A three-electrode cell set-up was utilized, with a saturated calomel electrode (SCE) as the reference electrode and a platinum electrode as the counter electrode. The open circuit potential (OCP) was recorded for 3600 s. Electrochemical Impedance Spectroscopy measurement (EIS) was performed from 10^5 Hz to 10^{-2} Hz, by applying 10 mV perturbation to OCP. The potentiodynamic polarization tests (PDP) were conducted at a scanning rate of 1 mV/s.

3. Results

3.1. Immersion test

Fig.

For Mg and CoCrMo, the effect of H_2O_2 on solution pH was indistinguishable, and H_2O_2 slightly affected their corrosion rate. Regarding Fe, H_2O_2 significantly affected pH values and raised it. Higher amount of H_2O_2 added, faster solution pH increased. Moreover, H_2O_2 remarkably promoted the Fe corrosion in a concentration-relevant manner.

3.2. Surface morphology after immersion

Fig. 2

The surface morphology of Mg and CoCrMo in PBS was barely affected by H_2O_2 , but H_2O_2 significantly changed the corrosion of Fe. The thick product layer was formed on Fe after 14-day immersion in PBS. With more H_2O_2 added, the amount of corrosion product decreased. In presence of 30.0 mM H_2O_2 , the dense product layer vanished, and the surface was partially covered with clusters of corrosion product.

3.3. Electrochemical measurements

The OCP of Mg in four solutions fluctuated, implying the formation and breakage of passive film [11], and was noticeably raised by 30.0 mM $\rm H_2O_2$. For Fe, 0.1 mM $\rm H_2O_2$ significantly changed OCP in PBS and 1.0 mM $\rm H_2O_2$ negatively shifted it. Regarding CoCrMo alloy, with more $\rm H_2O_2$ added, OCP shifted towards more positive direction.

The cathodic current and corrosion potential of Mg in PBS was reduced by 0.1 and 1.0 mM H_2O_2 , and the effect of 30.0 mM H_2O_2 was

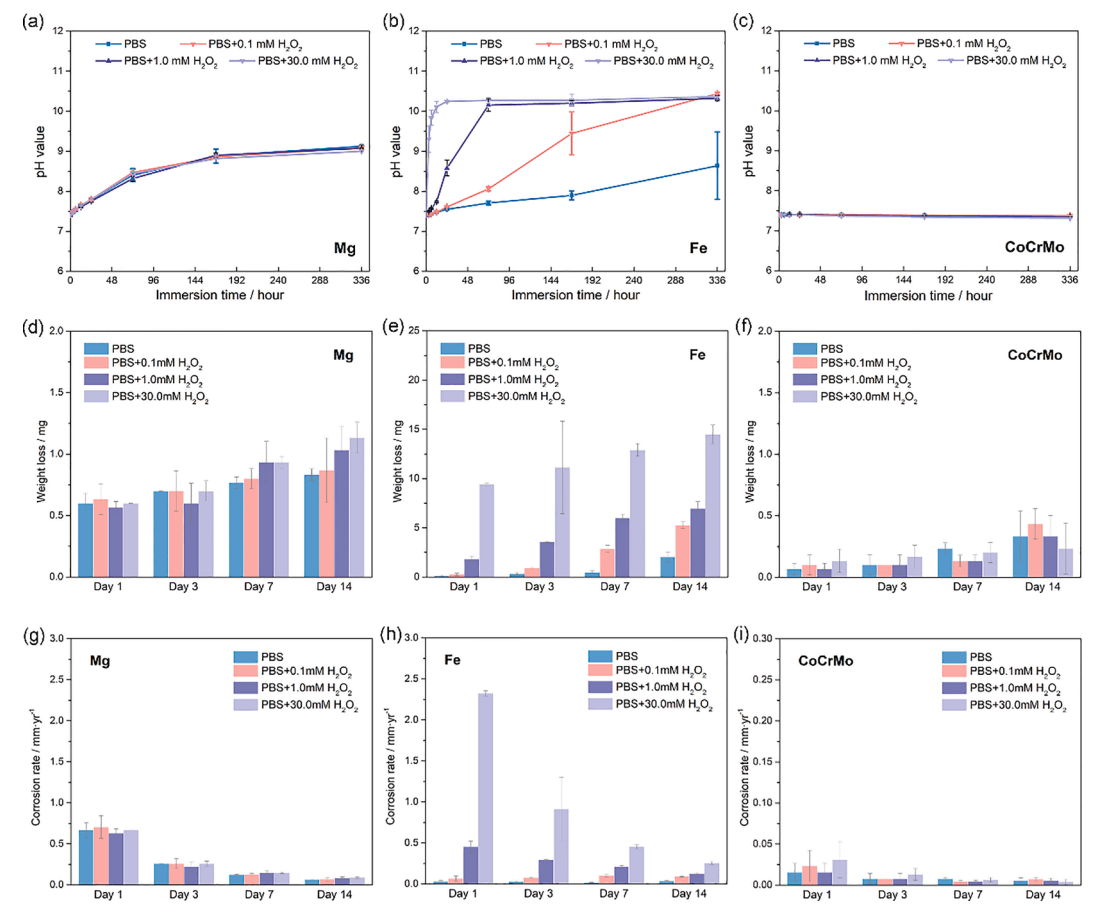


Fig. 1. Solution pH, weight loss and corrosion rate of Mg, Fe and CoCrMo.

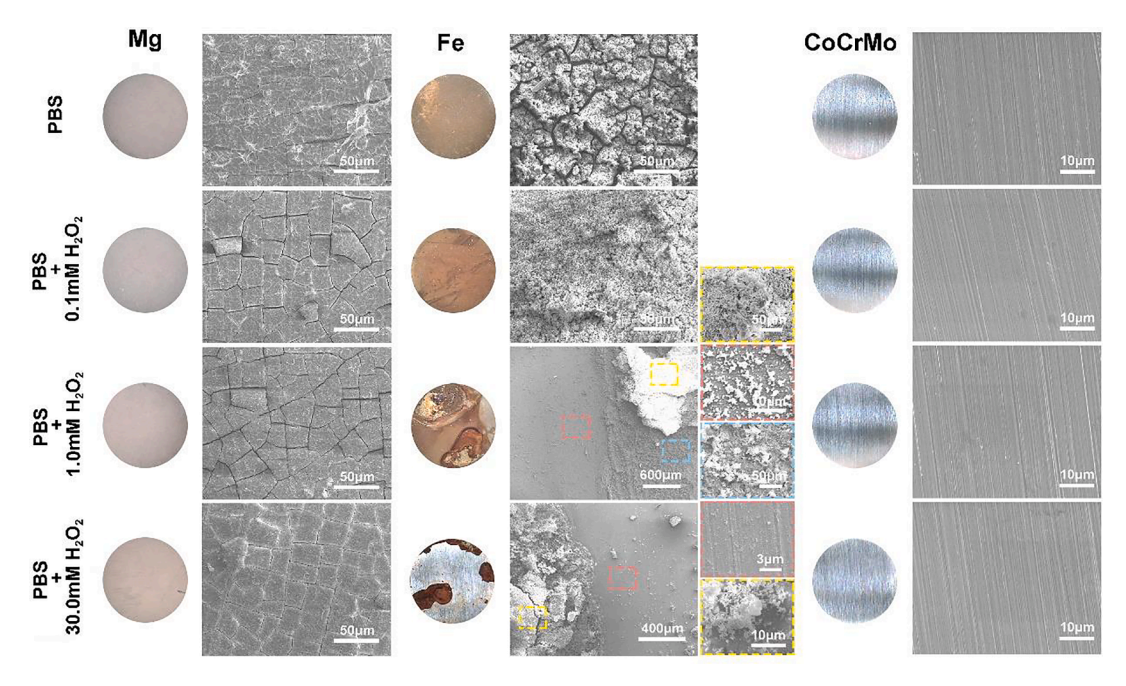


Fig. 2. The surface morphology of Mg, Fe and CoCrMo alloy after 14-day immersion.

indistinguishable. Regarding Fe, the corrosion potential was remarkably increased by $\rm H_2O_2$, and 30.0 mM $\rm H_2O_2$ notably accelerated cathodic and anodic reactions. The corrosion of Fe was stimulated by $\rm H_2O_2$ and a nearly thirty-fold increase in corrosion rate existed in presence of 30.0 mM $\rm \,H_2O_2$. Four PDP curves for CoCrMo alloy exhibited similar

 $\text{shapes} \cdot H_2O_2$ drifted the curve towards positive direction and delayed the corrosion.

Nyquist plots of Mg presented two capacitive loops and an inductive loop. The capacitive loop at high frequencies was assigned to charge transfer and double-layer/oxide film effects, and another one might be

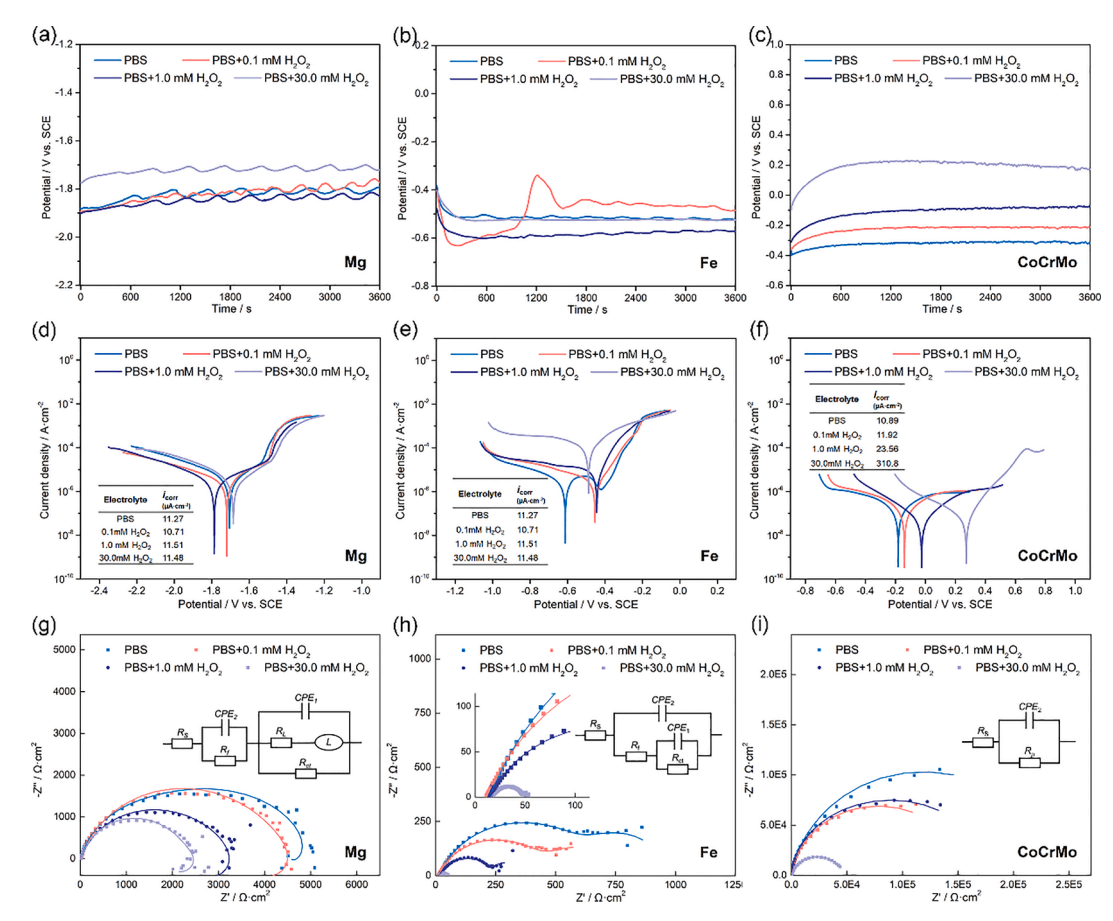


Fig. 3. OCP, PDP and EIS of Mg, Fe and CoCrMo alloy in simulated inflammatory solutions.

related with mass transport relaxation owing to diffusion of Mg^{2+} through the product layer [12]. The inductive loop might be attributed to the adsorption of Mg^+ intermediates [13]. $\mathrm{H_2O_2}$ reduced the dimension of nyquist plots of Mg in PBS. Nyquist plots of Fe consisted of two capacitive loops. The semicircle at high frequency described the faradaic charge transfer process and the other can be ascribed to the product layer [14]. With more $\mathrm{H_2O_2}$ added, nyquist plots exhibited smaller diameter. For CoCrMo alloy, the impedance response revealed high corrosion resistance of passive oxide film on the surface. The electrical equivalent circuits (EEC) were used to interpret the impedance response of Mg, Fe and CoCrMo. The scatter in Fig. 3 implied data points and the line fitted data.

4. Discussion

For Mg exposed to PBS, the dissolution of Mg takes place as the anodic reaction, and cathodic reaction involves the formation of hydrogen gas. The corrosion product was precipitated and the protective layer was formed, inhibiting the Mg corrosion, and lowering the corrosion rate. The oxidative environment in presence of H_2O_2 affected corrosion susceptibility of Mg in PBS, and changed its OCP and corrosion potential. The corrosion of Mg and CoCrMo under simulated inflammatory condition had certain features in common. The impedance response revealed reducing corrosion resistance of Mg and CoCrMo with more H_2O_2 present, and the effect of H_2O_2 on their corrosion during long-term immersion was insignificant. It's reported that the passive film was formed on CoCrMo in NaCl solution [15] and PBS, however, the oxide film morphology on CoCrMo can be changed by H_2O_2 . Moreover, OCP and corrosion potential increased, consistent with other studies [5,8], and exhibited a strong H_2O_2 concentration-dependent behavior.

Regarding Fe, the influence of H₂O₂ on its degradation was quite different. Fenton reactions might took place in presence of Fe ions and H₂O₂, produced reactive hydroxyl radicals and created the oxidizing environment [16]. The surface film behavior and OCP in PBS was changed in presence of H2O2. The EIS measurements revealed differently behaved surface film with H2O2 present, and the corrosion resistance of Fe decreased with increasing amount of H2O2. The cathodic and anodic reactions were accelerated by H2O2, and icorr increased immensely. In PBS, the dissolution of Fe is the anodic reaction, accompanied by the oxygen reduction as the cathodic reaction. The reduction of oxygen could take place via producing OH⁻ or H₂O₂, and the addition of H₂O₂ might influence the kinetics of both cathodic and anodic reactions. More importantly, it's deduced that H₂O₂ might promote the reduction of oxygen, and possibly H2O2 as well, which gave rise to a large amount of OH⁻, leading to increased solution pH [10], as well as the striking upsurge of corrosion rate. Therefore, the Fe degradation was remarkably accelerated and the formation of corrosion product was inhibited, especially in presence of 30.0 mM H₂O₂.

$$O_2 + 2H_2O + 4e^- \rightarrow 4OH^-$$
 (2)

$$Fe \rightarrow Fe^{2+} + 2e^{-} \tag{3}$$

$$Fe^{2+} + H_2O_2 \rightarrow Fe^{3+} + HO \bullet + OH^-$$
 (4)

5. Conclusion

In simulated inflammatory solutions, H_2O_2 changed the corrosion susceptibility and the oxide film behavior of pure Mg and CoCrMo alloy for the initial exposure in PBS, but slight affected their corrosion during long-term immersion. For Fe, the addition of H_2O_2 altered the surface film properties of Fe, significantly inhibited the precipitation of corrosion product, and accelerated its corrosion in a concentration-dependent way. The importance of taking inflammation-induced corrosion into consideration during the evaluation of biodegradable metal, in particular Fe, was thus highlighted.

CRediT authorship contribution statement

Xiao Liu: Conceptualization, Methodology, Investigation, Writing – original draft, Data curation. **Wenting Li:** Investigation. **Yan Cheng:** Investigation. **Yufeng Zheng:** Conceptualization, Methodology, Resources, Supervision, Writing – review & editing, Project administration, Funding acquisition.

Declaration of Competing Interest

The authors declare that they have no known competing financial interests or personal relationships that could have appeared to influence the work reported in this paper.

Acknowledgements

This work was supported by National Natural Science Foundation of China (Grant No. 51931001), and International Cooperation and Exchange project between NSFC (China) and CNR (Italy) (NSFC-CNR Grant No. 52011530392).

References

- [1] H.-S. Han, S. Loffredo, I. Jun, et al., Mater. Today 23 (2019) 57-71.
- [2] Y.F. Zheng, X.N. Gu, F. Witte, Mater. Sci. Eng.: R: Rep. 77 (2014) 1–34.
- [3] Y. Zhang, O. Addison, F. Yu, et al., Sci. Rep. 8 (1) (2018) 3185.
- [4] J.L. Gilbert, S. Sivan, Y. Liu, et al., J. Biomed. Mater. Res. A 103 (1) (2015) 211–223.
- [5] Y. Liu, J.L. Gilbert, J. Biomed. Mater. Res. Part B: Appl. Biomater. 106 (1) (2018) 209–220.
- [6] Y. Liu, J.L. Gilbert, Wear 390-391 (2017) 302-311.
- [7] T. Hui, G.W. Kubacki, J.L. Gilbert, J. Biomed. Mater. Res. A 106 (1) (2018) 160–167.
- [8] Y. Liu, J.L. Gilbert, Electrochim. Acta 262 (2018) 252-263.
- [9] Assis, S.L. de, Costa, et al., Mater. Res. (2006).
- [10] E. Scarcello, D. Lison, J. Funct. Biomater. 11 (2019) 1.
- [11] S. Naddaf Dezfuli, Z. Huan, J.M.C. Mol, et al., Prog. Nat. Sci.: Mater. Int. 24 (5) (2014) 531–538.
- [12] M. Ascencio, M. Pekguleryuz, S. Omanovic, Corros. Sci. 87 (2014) 489-503.
- [13] N. Pebere, C. Riera, F. Dabosi, Electrochim. Acta 35 (2) (1990) 555–561.
- [14] M. Mouanga, P. Berçot, Corros. Sci. 52 (12) (2010) 3993-4000.
- [15] A.W.E. Hodgson, S. Kurz, S. Virtanen, et al., Electrochim. Acta 49 (13) (2004) 2167–2178.
- [16] S.A.M. Ali, P.J. Doherty, D.F. Williams, J. Appl. Polym. Sci. 51 (8) (1994) 1389–1398.